THE ASTROPHYSICAL JOURNAL, 281:L25–L28, 1984 June 1

INTERPRETATION OF THE NUMBER VERSUS DIAMETER DISTRIBUTION FOR SUPERNOVA REMNANTS IN THE LARGE MAGELLANIC CLOUD

JOHN P. HUGHES, DAVID J. HELFAND, AND STEVEN M. KAHN
Columbia Astrophysics Laboratory, Columbia University
Received 1983 October 31; accepted 1984 February 23

ABSTRACT

We have examined the cumulative number versus diameter relation for an X-ray selected sample of supernova remnants in the Large Magellanic Cloud in an attempt to understand the evolutionary state of these objects. Previous studies have suggested that the observed linear $N(D)$ relation requires the remnants in the cloud to be freely expanding. We have carried out detailed calculations to determine the effect of a luminosity threshold on the observed distribution and show that the observations can be fitted by remnants which are in the adiabatic or later stages of evolution. We discuss the implications of our results for the supernova creation rate in the LMC.

Subject headings: galaxies: Magellanic Clouds — nebulae: supernova remnants

I. INTRODUCTION

Observations of supernova remnants (SNRs) in external galaxies can serve as an important probe of the statistical properties of SNRs as a class. The Large Magellanic Cloud (LMC) is ideally suited for such study because of its close proximity to the Galaxy (55 kpc; Bok 1966) and moderate size ($\sim 10^{10}\ M_\odot$), and indeed it has been extensively surveyed at almost all wavelengths. An X-ray survey (Long, Helfand, and Grabelsky 1981) was recently carried out by the imaging proportional counter (IPC) on board the *Einstein* satellite (Giacconi *et al.* 1979). This complete IPC survey of LMC X-ray sources listed a total of 26 SNRs and suggested 11 other candidates; a further, approximately 30 sources remain unidentified (Helfand 1984). Mathewson *et al.* (1983) present a summary of recent observations for the 25 confirmed LMC SNRs which includes radio flux densities and spectral indices and X-ray luminosities from the IPC observations, as well as optical photographs and X-ray contour maps, many produced by the high resolution imager (HRI) on board *Einstein*.

In this *Letter* we have considered the $N(D)$ relation for the sample of SNRs given by Mathewson *et al.* (1983). We have combined their Type I and Type II remnants into one group and have excluded the three centrally condensed remnants, N158A, N157B, and N103B, from the sample. Observations using the HRI, the IPC, and the solid state spectrometer (SSS) (Clark *et al.* 1982) show marked differences in the morphological and spectral characteristics of the X-ray emission from these objects. They most probably belong to the class of Crablike remnants for which evolutionary behavior is governed by the spindown of a central neutron star rather than by the dissipation of a supernova shock, and they will not be considered further here. Reapplying the maximum likelihood method (Crawford, Jauncey, and Murdoch 1970) to the remaining sample of 21 objects detected by the IPC, we obtain $N(<D) = 0.206\ D^{+1.15 \pm 0.29}$. A similar, approximately linear dependence on diameter had been found previously for radio selected SNRs (Clarke 1976; Mills 1984).

These authors, and others, have chosen to interpret this result as implying that the LMC remnants are still in the free expansion phase of evolution out to diameters of approximately 40 pc. We review this argument below. However, this conclusion has been drawn without careful consideration of the selection effects (such as surface brightness or luminosity thresholds, or both) which went into the construction of the samples. SNRs which are formed with different initial explosion energy (E_0) and in regions of differing interstellar medium density ($n_{\rm ISM}$) will have different luminosities when they have evolved to the same diameter. Thus these remnants will have different diameters when they have reached or fallen below a given limiting luminosity. This means that a luminosity (or surface brightness) detection threshold will be important, not only at the large diameter limit of the survey, but throughout the range of diameters sampled. Consequently, the $N(D)$ relation can be used to constrain the actual underlying physical distribution of SNRs only when a diameter-dependent luminosity threshold is properly included in the analysis.

In § II we begin by reviewing the expected form of the $N(D)$ relation for various stages of SNR evolution in the absence of diameter-dependent thresholds. We then show analytically how the calculation is modified when SNRs with a distribution of values for $n_{\rm ISM}$ and E_0 are included in a survey with a finite surface brightness or luminosity threshold. In § III, we employ a grid of one-dimensional hydrodynamic models to determine the diameter-dependent luminosity threshold and to establish the extent of the effect such a threshold has on the sample of LMC remnants cataloged by Mathewson *et al.* (1983); we show that a linear $N(D)$ relation is consistent with Sedov evolution and a reasonable range of supernova explosion energies and interstellar medium densities. The final section summarizes our results, and we comment on the SNR creation rate in the LMC.

II. X-RAY DETECTION THRESHOLDS AND THE $N(D)$ RELATION: AN ANALYTIC TREATMENT

A theoretical $N(D)$ relation can be determined using

$$\frac{dN}{dD} = \int dt \frac{dN}{dt} \iint \cdots \int d\xi_1 \, d\xi_2 \cdots d\xi_n \, f(\xi_1) g(\xi_2) \cdots h(\xi_n) \times \delta[D - D(t, \xi_1, \xi_2, \ldots, \xi_n)], \quad (1)$$

where $\xi_1, \xi_2, \ldots, \xi_n$ are the parameters governing the assumed type of SNR evolution, $f, g, \ldots, h$ are the distribution functions for these parameters, dN/dt is the SNR creation rate, and $\delta[D - D(t, \xi)]$ is used to select the relationship between the diameter D and time t appropriate to a given type of evolution. In the absence of a diameter-dependent luminosity threshold, the integration limits for the evolution parameters are, at least formally, 0 to ∞. For remnants in the free expansion phase of evolution, age scales linearly with diameter, $t = D/2V_{\text{ex}}$, where V_{ex} is the speed with which the outer layers of the supernova star are ejected. Assuming a constant supernova rate and a narrow range of expansion velocities, we obtain $N(D) \sim D^1$. Introducing Sedov evolution into equation (1) using the well-known similarity solution (Sedov 1959), $t = 2.7\,(n_{\text{ISM}}/E_{51})^{1/2} D_{\text{pc}}^{5/2}$ yr, where E_{51} is E_0 in units of 10^{51} ergs, we obtain $N(D) \sim D^{5/2}$, again in the absence of a detection threshold. Note that for both of these evolutionary tracks, there is only one parameter governing the evolution, either V_{ex} or n_{ISM}/E_{51}.

In the presence of a diameter-dependent luminosity threshold the integration limits for the evolution parameters in equation (1) become functions of the diameter and perhaps the other parameters, $\xi_i = \xi_i(D, \xi_j), j \neq i$, expressing the fact that there are regions of the available parameter space which were not surveyed. For example, with Sedov evolution parameterized by the single quantity $\xi \equiv n_{\text{ISM}}/E_{51}$ and including luminosity thresholds, the cumulative number relation can be expressed as

$$N(D') = 6.8\, R_{\text{SNR}} \int_0^{D'} dD\, D^{3/2} \int_0^{\xi(D)} d\xi\, \xi^{1/2} f(\xi), \quad (2)$$

where R_{SNR} is the SNR creation rate per year, assumed constant.

The diameter-dependent luminosity threshold is a functional relationship between the SNR evolution parameters and the maximum observable diameter. At the most basic level, however, the diameter-dependent luminosity threshold is determined by how the softening of the emergent X-ray spectra from SNRs as they age and cool depends on n_{ISM} and E_0. However, it will involve details of the instrument response, the SNR X-ray spectrum, the SNR dynamics, etc. In order to properly include these details, of which, in particular, the effects of radiative cooling on the diameter evolution and the finite bandwidth of the survey instrument are most important, it is necessary to perform a numerical calculation. We present the results of such a calculation in the next section.

III. X-RAY DETECTION THRESHOLDS AND THE $N(D)$ RELATION: NUMERICAL MODELS

We have used a one-dimensional, spherically symmetric, hydrodynamic shock code to model the temperature and density evolution of SNRs (see White and Long 1983 for details). We include radiative cooling and allow the electron and ion temperatures to come to equilibrium through Coulomb collisions. Most of our runs were produced using a $\frac{1}{2}\,M_\odot$ uniform density, uniform velocity shell of ejecta; two runs were done using an ejecta of 5 $M_\odot$, but the results, for our purposes here, were consistent with those using lower mass ejecta in that the maximum diameters reached were approximately the same. We neglect magnetic fields and inhomogeneities in the surrounding medium; neither are expected to be critical at the phases of evolution most relevant to the present discussion.

We have used this code to examine a set of model SNRs with ranges of E_{51} from 0.01 to 10.0 and n_{ISM} from 0.1 cm^{-3} to 10.0 cm^{-3}. The evolution of each remnant was followed to an age of 10^5 years, or until the shock diameter was greater than 50 pc. In general, our models follow the usual evolutionary scenario: from the free expansion phase (where radius increases with time as $r \sim t^1$) into the Sedov or adiabatic phase (where $r \sim t^{0.4}$), and finally into the radiative phase (where $r \sim t^{0.3-0.25}$). However some models, namely those with the lowest densities, never reach the radiative phase within the age constraints of the calculation.

The luminosity of each model as a function of age was calculated from the temperature and density profile integrated over the volume of the remnant. The temperature in each radial bin determined the volume emissivity, which we assumed to be that of a Raymond and Smith (1977) thermal plasma with standard cosmic metal abundances and equilibrium ionization.[1] We then convolved our model source spectra with the latest versions of the IPC spectral response matrix and the on-axis effective area function to determine an IPC count rate for each model as a function of time. Corrections for interstellar absorption using the cross sections from Brown and Gould (1970) were included for two values of hydrogen column density, $10^{20.5}$ cm^{-2} and 10^{21} cm^{-2}, which represent the range of total absorption along the line of sight, including absorption in our Galaxy (Heiles and Cleary 1979) as well as the LMC itself (McGee and Milton 1963). We set our luminosity limit at 0.01 IPC counts s^{-1}, the approximate limit of the X-ray survey (Long, Helfand, and Grabelsky 1981), and used a distance to the LMC of 55 kpc (Bok 1966). We then determined the diameter-dependent luminosity threshold as a function of the model parameters, n_{ISM} and E_{51}. This result is displayed in Figure 1 for a column density of

[1] This is, of course, a rather naive approach to take during all the stages of evolution of a model remnant, but for our purposes it serves as a quite reasonable approximation. We wish to know when a remnant falls below the luminosity threshold of the survey; in general, this will occur when a remnant is at or approaching the radiative phase. At the age where this occurs, the X-ray luminosity comes from the volume interior to the dense shell, where the hot, fairly low density, swept-up matter (of presumably cosmic abundance, since the mass of ejecta is negligible by now) has had sufficient time to reach ionization equilibrium.

$10^{20.5}$ cm^{-2}, where a tight anticorrelation is seen to exist between the ratio of $\xi = n_{\rm ISM}/E_{51}$ and the maximum diameter, $D_{\rm pc}$, to which a remnant in the LMC is observable. A least squares fit minimizing $\Sigma[\xi_i - \xi(D_i)]^2$ yields the relation $\xi = 1.55 \times 10^5 D_{\rm pc}^{-2.95}$. The higher column density results are similar, with $\xi = 8.52 \times 10^4 D_{\rm pc}^{-2.90}$, but the maximum diameters reached are smaller, as expected.

We have numerically integrated equation (2) using various forms of the ξ distribution (lognormal, power law, and exponential), and have compared the model $N(D)$ relations obtained to the observed one using the Kolmogorov statistic. The two distributions are each normalized to lie between 0 and 1, and the maximum unsigned difference between them is determined. For a sample of size 21, there is a 10% probability (1.65 σ) that the maximum deviation between the cumulative distributions of the models and the sample exceeds 0.26 (Birnbaum 1952). In the sense of this test we have obtained acceptable fits for a large range of parameters. However, we expect and have confirmed that we are actually not sensitive to the assumed distribution for ξ outside the range from roughly 0.1 to roughly 100. The relative contribution to the model distribution from remnants with $\xi \lesssim 0.1$ decreases with decreasing ξ because of the $\xi^{1/2}$ factor in equation (2). Our insensitivity to remnants with $\xi \gtrsim 100$ arises because these SNRs fall below the survey detection threshold at increasingly smaller diameters with increasing ξ, and hence contribute to

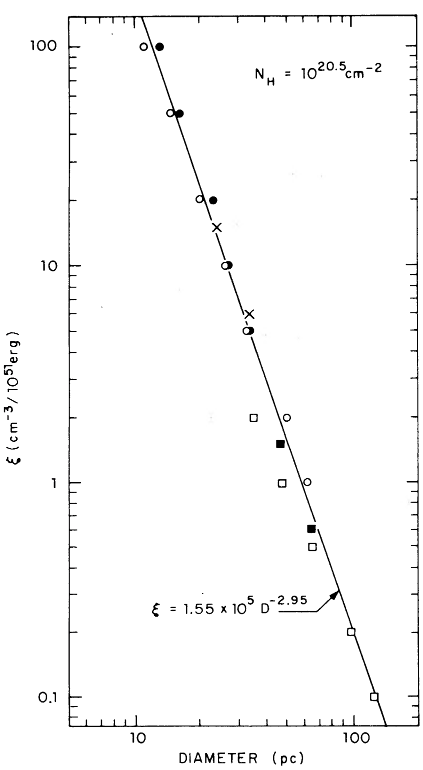

FIG. 1.—Maximum observable diameter vs. $\xi = n_{\rm ISM}/E_{51}$ for a set of SNR models at the distance of the LMC with an interstellar absorption of $10^{20.5}$ H atoms cm^{-2}. The different symbols correspond to the different $n_{\rm ISM}$ values used in the models: *open squares*, 0.1 cm^{-3}; *filled squares*, 0.3 cm^{-3}; *open circles*, 1.0 cm^{-3}; $\times$, 3.0 cm^{-3}; and *filled circles*, 10. cm^{-3}.

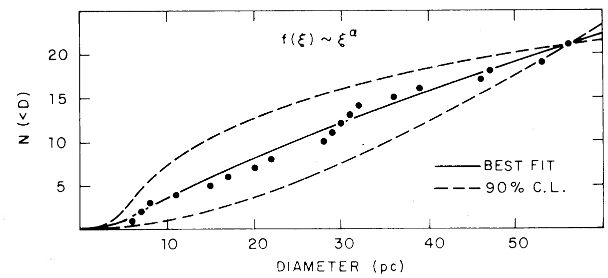

FIG. 2.—Model number vs. diameter relations for a sample of Sedov remnants, using a power-law distribution for ξ with upper and lower cutoffs of 10^3 and 10^{-2}. The filled circles are the X-ray data, the dashed curves correspond to the 90% confidence level limits (*upper*: $\alpha = -0.7$, *lower*: $\alpha = -1.3$), and the solid curve is the best fit ($\alpha = -0.9$).

the $N(D)$ relation only at small diameters. For $\xi > 10^4$, the maximum diameter corresponds to $D < 2$ pc. Thus high and low values of ξ cannot influence the shape of the model $N(D)$ relation, only its overall normalization.

We have chosen to present only the results of our power-law fits to the ξ distribution function, where we have taken upper and lower limits to the distribution of 10^3 and 10^{-2}.[2] The 90% confidence level limits for the power-law indices using either value of hydrogen column density are -0.7 to -1.3. Figure 2 presents the calculated model $N(D)$ distribution for Sedov remnants using the best fit power-law index and the 90% confidence level limits superposed on the observed distribution of LMC SNRs. We have also examined SNR dynamical evolutions corresponding to post–Sedov type evolution, such as radiative phase evolution (as in Chevalier 1974) or constant radial momentum (Oort 1951); the results for the distribution of ξ are consistent with those given above.

The value for $R_{\rm SNR}$ obtained from normalizing the model distribution to the observed one depends on the power-law index used; we include this by giving the average value of $R_{\rm SNR}^{-1}$ and errors which express the variation over the quoted range of power-law indices. These values for the average interval between remnant-producing supernova explosions in the LMC are 800 $\pm$ 200 years ($n_{\rm H} = 10^{21}$ H atoms cm^{-2}) or 1000 $\pm$ 200 years ($n_{\rm H} = 10^{20.5}$ H atoms cm^{-2}).

IV. SUMMARY AND CONCLUSIONS

Our principal conclusion regards the evolutionary state of the SNRs in the LMC. We have demonstrated, using reasonable assumptions and carefully examining the survey criteria, that these remnants can be described by the usual standard evolutionary scenarios for intermediate and old age remnants, such as Sedov type evolution or the dense shell formation

[2] On the basis of the statistical test, alone, however, we are unable to constrain the actual range of ξ required for acceptable fits. In fact, a δ-function distribution for ξ which peaks anywhere from $\xi = 2.0$ to 4.0 or, for example, a power-law distribution for ξ ($\alpha \sim -1.0$) with an upper limit of 4.0 and lower limit of 1.0 both give maximum deviations which are less than 0.26. Nevertheless, we question the physical validity of such narrow ranges for the ratio of $n_{\rm ISM}$ to E_{51} and have restricted our analysis to determining the power-law index for set upper and lower limits to the ξ distribution.

stage of evolution as discussed in § III. Thus the linear $N(D)$ relation observed for the X-ray sample of LMC remnants should be viewed as consistent with, but certainly not as requiring, that the majority of these SNRs are freely expanding.

We also present a lower limit to the SNR creation rate in the LMC of about one explosion every 1000 years. This is a lower limit for several reasons. The first is a result of geometric effects, namely departures from spherical symmetry, which tend to decrease the luminosity from an actual remnant by an amount depending on the filling factor of the emitting gas. By including filling factors ranging from 0.1 to 1 in our simulations, we have estimated that this effect will decrease the calculated interval between supernova explosions by only about 20%–30%. Second, the X-ray survey is not complete for large-diameter remnants nor for the whole of the LMC to the flux limit used (Helfand 1984). Finally, observations of galactic remnants, where two of the seven historical remnants fall below the detection threshold of the LMC survey (Pisarski, Helfand, and Kahn 1984), imply that there are regions of the parameter space of n_{ISM} and E_{51} which were not sampled by the IPC survey of the LMC.

We acknowledge helpful discussions with Gary Chanan. This work was supported by the National Aeronautics and Space Administration under contract NAS 8-30753 and by the United States Air Force under grant AFOSR 82-0014. This article is Columbia Astrophysics Laboratory Contribution No. 257.

REFERENCES

Birnbaum, Z. W. 1952, *J. Am. Stat. Assoc.*, **47**, 425.
Bok, B. J. 1966, *Ann. Rev. Astr. Ap.*, **4**, 95.
Brown, R. L., and Gould, R. J. 1970, *Phys. Rev. D*, **1:8**, 2252.
Chevalier, R. A. 1974, *Ap. J.*, **188**, 501.
Clark, D. H., Tuohy, I. R., Long, K. S., Szymkowiak, A. E., Dopita, M. A., Mathewson, D. S., and Culhane, J. L. 1982, *Ap. J.*, **255**, 440.
Clarke, J. N. 1976, *M.N.R.A.S.*, **174**, 393.
Crawford, D. F., Jauncey, D. L., and Murdoch, H. S. 1970, *Ap. J.*, **162**, 405.
Giacconi, R., *et al.* 1979, *Ap. J.*, **230**, 540.
Heiles, C., and Cleary, M. N. 1979, *Australian J. Phys. Ap. Suppl.*, **47**, 1.
Helfand D. J. 1984, in *IAU Symposium 108, Structure and Evolution of the Magellanic Clouds*, ed. K. de Boer and S. van den Bergh (Dordrecht: Reidel), in press.
Long, K. S., Helfand, D. J., and Grabelsky, D. A. 1981, *Ap. J.*, **248**, 925.
Mathewson, D. S., Ford, V. L., Dopita, M. A., Tuohy, I. R., Long, K. S., and Helfand, D. J. 1983, *Ap. J. Suppl.*, **51**, 345.
McGee, R. X., and Milton, J. A. 1963, in *IAU Symposium 20, The Galaxy and The Magellanic Clouds*, ed. F. J. Kerr and A. W. Rodgers (Canberra: Australian Acadamy of Sciences), p. 126.
Mills, B. Y. 1984, in *IAU Symposium 108, Structure and Evolution of the Magellanic Clouds*, ed. K. de Boer and S. van den Bergh (Dordrecht: Reidel), in press.
Oort, J. H. 1951, *Problems of Cosmical Aerodynamics* (Dayton, Ohio: Central Air Document Office).
Pisarski, R. L., Helfand, D. J., and Kahn, S. M. 1984, *Ap. J.*, **277**, 710.
Raymond, J. C., and Smith, B. W. 1977, *Ap. J. Suppl.*, **35**, 419.
Sedov, L. I. 1959, *Similarity and Dimensional Methods in Mechanics* (New York: Academic Press).
White, R. L., and Long, K. S. 1983, *Ap. J.*, **264**, 196.

David J. Helfand, John P. Hughes, and Steven M. Kahn: Columbia Astrophysics Laboratory, Departments of Astronomy and Physics, Columbia University, 538 West 120th Street, New York, NY 10027